Dimensional Analysis and Mechanical Properties Characterization of Carbon Nanofibers under Subzero Temperatures

Zhuxin Dong, *Member, IEEE*, Uchechukwu C. Wejinya, *Member, IEEE*, Siva Naga Sandeep Chalamalasetty, *Member, IEEE*, and M. Meyyappan, *Fellow, IEEE*

***Abstract*—The ability of carbon nanofibers grown on nanoelectrode chips for ultrafast detection of molecules down to parts per billion (ppb) with a response time in seconds and with a minimal usage of power has attracted the attention of materials researchers and nanotechnology explorers—for example, space research organizations. Application in chemical and biological sensing is being studied extensively. NASA in their report on failure of space missions released in 2008 emphasized on the need for studying extreme environmental behavior of futuristic space materials. Very little work has been done to understand the behavior of the nanofibers operating in low-temperature environments. In this paper, vertically aligned carbon nanofibers (VACNFs) have been characterized for their survival in extreme low-temperature environments using a combination of environmental chamber and atomic force microscopy (AFM). Specifically, this paper characterizes through nanoindentation the mechanical properties and dimensional stability of VACNFs operating in low-temperature environments.**

***Index Terms*—Atomic force microscopy (AFM), carbon nanofibers, mechanical properties, nanoindentation, subzero.**

I. Introduction

A MAJOR concern for the space organizations is to adjust the space and resources available on a space mission. Extraordinary electro mechanical properties of carbon nanomaterials had attracted the attention of researchers [1]–[3]. Ever since discovery of carbon nanotubes [4], researchers have effectively used them as sensory materials, storage materials, hardening materials etc. [5]–[16]. With the advancement in MEMS technologies and understanding about carbon nanomaterials integration, today it is possible to detect molecules down to parts per billion (ppb) with carbon nanomaterials sensors [17], [18]. More exciting are their response time in seconds and the resources in millivolts. Thus, many space research organizations, for example NASA, are exploring the possibility of integration of sensors made of carbon nanomaterials.

NASA took the initiative and established the Center for Nanotechnology at NASA Ames Research Center with a mission "To develop nanotechnology-based chemical sensors that can provide high-sensitivity, low-power, and low-cost portable tools for *in situ* chemical analysis in space and terrestrial applications" [19]. The general scientific and technical importance for the establishment of the Center for Nanotechnology lies in the fact that the developed nanosensor platform is suitable for detecting gases and volatile organic compounds, and can be used for chemical analysis in both gas and liquid phases. Nanochemical sensors will significantly improve scientific measurement capability for earth and space science. Combined with MEMS technology, light and compact sensors can be made in wafer scale with low cost, which including higher sensitivity and lower power consumption makes the sensor suitable in long duration missions. The center has reported carbon nanotube-based sensors that offer very high sensitivity for NO_2, ammonia, methane, acetone, benzene, and toluene detection, with detection limits in the lower ppm to ppb level and response time in seconds to minutes [19]. Each sensor draws the power in microwatts to milliwatts. The size of the detector is designed to be $5' \times 5' \times 1'$ for 32 sensing elements detection system. The weight of this detector is estimated to be less than 2 kg. All these factors are encouraging scientists to use them in space applications. However, performance of the sensing elements in extraordinary conditions has to be calibrated before practical space applications.

In 2003, the Nuclear Regulatory Committee (NRC) Decadal Survey for Solar System Exploration recommended that "NASA commit to significant new investments in advanced technology so that future high–priority flight missions can succeed." In a 2007 report released by NASA [20] on its failure of flight missions, it concluded that extreme environments of temperature, pressure, and extreme radiations are the primary causes for the failure of the missions. The report also emphasizes on the need for investment on extreme environment technology needs. In the near future, there will be many more outer space missions, and this pose a greater challenge to the scientific community for development of materials that can cater the needs of these missions.

Manuscript received January 8, 2012; revised January 17, 2013 and May 17, 2013; accepted July 19, 2013. Date of publication July 24, 2013; date of current version September 4, 2013. This work was supported in part by the University of Arkansas, College of Engineering External Mentoring Award Program. The review of this paper was arranged by Associate Editor L. Dong

Z. Dong was with the Department of Mechanical Engineering, University of Arkansas, Fayetteville, AR 72701 USA. He is now with the Department of Civil and Environmental Engineering and Earth Sciences, University of Notre Dame, Notre Dame, IN 46556 USA (e-mail: zdong1@nd.edu).

U. C. Wejinya is with the Department of Mechanical Engineering, University of Arkansas, Fayetteville, AR 72701 USA (e-mail: uwejinya@uark.edu).

S. N. S. Chalamalasetty was with the Microelectronics and Photonics Graduate Program, University of Arkansas, Fayetteville, AR 72701 USA. He is now with Micron Technology Inc., Manassas, VA 20110 USA (e-mail: schalama@uark.edu).

M. Meyyappan is with the Center for Nanotechnology, NASA Ames Research Center, Moffett Field, CA 94035 USA (e-mail: m.meyyappan@nasa.gov).

Color versions of one or more of the figures in this paper are available online at http://ieeexplore.ieee.org.

Digital Object Identifier 10.1109/TNANO.2013.2274519

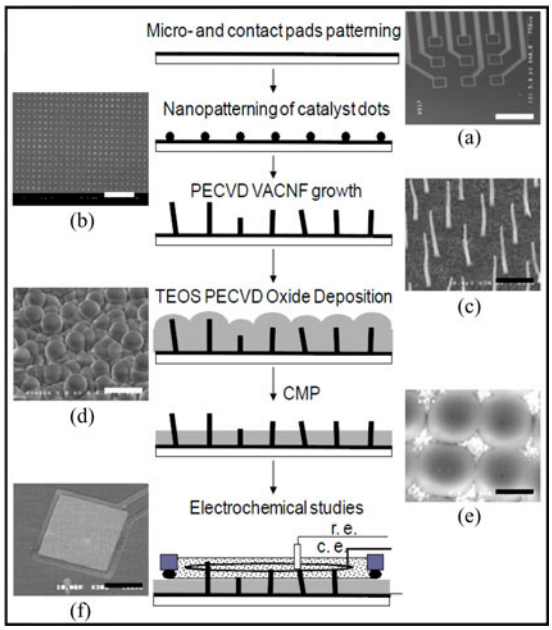

Fig. 1. Fabrication steps and the changes on the wafer can be seen in the pictures in-sight. (a) deposition of metal, (b) nanopatterning, (c) growth of CNFs, (d) deposition of silicon dioxide, (e) chemical mechanical polishing, and (f) wet etch. The scale bars in (a) to (f) are 705, 5, 1, 3, 0.67, and 100 μm respectively.

The fact that most of our planetary system is engulfed in negative temperature convinces us to characterize the nanofibers at subzero temperatures. And more over since the mechanical properties of the materials change widely with temperatures, mechanical property measurement is targeted.

II. Materials and Methods

A. Fabrication of Nanoeletrode Array

NASA Ames Research Center has helped us by supplying the vertically aligned carbon nanofibers (VACNFs) nanoelectrode arrays (NEA) [21], and it includes six major steps done on a 4 in silicon <100> wafer that is previously coated with 500 nm of silicon dioxide. The fabrication process is shown in Fig. 1, and the steps include 1) metal deposition; 2) nanopatterning of Ni catalyst dots; 3) directional growth of CNFs; 4) silicon dioxide deposition for electrical isolation and mechanical support; 5) chemical mechanical polishing (CMP) to expose CNF tips, and 6) a wet etch with 7:1 HF to expose contact pads.

1) Deposition of Metal: In this step metal is deposited for micropads, contact pads, and interconnects. A single 4-in Si wafer is lithographically patterned for nine micropads, nine contact pads, and channels for interconnects. This patterned structured is inspected microscopically and then electron beam evaporation is compression, exercised to deposit a 200-nm thick Cr film and then the wafer is immersed in acetone for one hour. Once removed from the acetone, the wafer is sprayed with methanol and isopropyl alcohol and blown dry with N_2.

2) Nanopatterning of Ni-Catalyst Dots: Using e-beam lithography, Ni dots are patterned onto the substrate. Approximately ~39 000 Ni catalyst dots are patterned onto each of the micropads. A 400-nm-thick Poly(methyl methacrylate) (PMMA) A7 was spun coated at 3000 r/min, baked at 180 °C for 90 s, and exposed at 100 keV, 2 nA, 1950 μC/cm^2. Exposures were developed in a solution of 1:1methyl isobutyl ketone (MIBK): IPA for 2 min, immersed in IPA for 30 s, and blown dry with N_2. Subsequently, the patterned catalyst dots are verified using an optical microscope and a 10-nm Cr followed by 30-nm Ni catalyst were deposited by electron beam evaporation at ~2 Å/s. The coated wafers were immersed in acetone for 1 h. The wafers were then removed from the acetone while being sprayed with IPA and then blown dry with N_2.

3) Directional Growth of VACNFs: The next step is directional growth of VACNFs on the nickel dots that were created in step B. A dc-biased PECVD is employed at a processing pressure of 6.3 mBar, plasma power of 180 W and 700 °C, 125 sccm C_2H_2 feedstock and 444 sccm NH_3 diluents were initiated. Then a 5 min thermal annealing at 600 °C is carried out before initiating the plasma with 250 sccm NH_3. To attain the required growth temperatures and thermal anneal, a 60 °C/min thermal gradient was used. Each individual CNF is vertically arranged to free stand on the surface with Ni catalyst on each tip. Operating deposition for 15 min has produced CNFs of height 1.5 μm, base diameter 100 nm, and tip diameter 70 nm on average. At this step Scanning Electron Microscopy (SEM) is used to validate the results.

4) Deposition of Silicon Dioxide: In order to passivate the side walls of nanofibers, a 3 μm $\pm$ 0.8% of SiO_2 layer is deposited onto the wafers using a pressure of 3 Torr, temperature of 400 °C and RF power of 1000 W. A mixture of ~6000 sccm of O_2 and 2–3 mL/min of tetraethyl orthosilicate (TEOS) is used in a parallel plate dual RF PECVD to obtain highly conformal coating of SiO_2 on newly created nanofibers and interconnects.

5) Chemical Mechanical Polishing: Surface polarization along with exposing the nanofiber tips is attained by removal of excess SiO_2 and partial removal of nanofiber tip using Chemical Mechanical Polishing (CMP). This process involves removing the existing material with 0.5-μm alumina (pH 4) at 10 mL/min, 60-r/min platen, 15-r/min carrier, and 15 psig down force at 150 nm/min for irrefutable polishing. Wafer was then cleaned by immersing it into a solution composed of water, hydrogen peroxide, and ammonium hydroxide at a ratio of 80:2:1, respectively, and then spin-dried.

6) Wet Etch: This is the final step in the fabrication of VACNFs. In general wet etch is used for exposure of contact pads which are covered with SiO_2. A 7:1 diluted HF solution is expended to etch oxide ~15 Å/s. Wafers are then diced for individual chips.

B. Extreme Environment Treatment

The fabricated chips are now subjected to extreme environments in a controlled environmental chamber. For this purpose, a microclimate environmental chamber (Cincinnati Sub Zero, model No. MCBH 1.3) is used. With an error of $\pm$0.5% in the range of -70 °C to 190 °C, the data of temperatures is precise and accurate. In this method, the environmental chamber is set to a fixed temperature. After the attainment of the specified

temperature, the substrate with nanofibers is placed in the environmental chamber for 30 min at the specified temperature in order to facilitate response to temperature. Then, the substrate is transferred into a dry box (McDry, MCU-201) for about 90 s to eliminate water vapor. The relative humidity of dry box normally remains as low as 1% in normal operation. After loading the sample from the subzero temperature treatment chamber, the percentage can return to less 3% in 90 s. Then, the sample can be transferred to the AFM for imaging to measure the dimensions and analyze the mechanical properties of treated fibers. In general, it takes about 255 s to complete a single frame scan for a 5 μm $\times$ 5 μm area as the scan speed is set at 5.021 μm/s, which means 1.004 line/s, and the image resolution is 256 $\times$ 256.

C. Atomic Force Microscopy

The subjected samples are analyzed for dimensional changes and mechanical fatigue using Atomic Force microscopy (Agilent 5500 ILM, Agilent Technologies, Inc., Santa Clara, CA, USA). Scanning Electron Microscope (SEM) is also employed to further validate the nanofibers.

1) Scanning and Measurement: AFM is used for accurate measurement of fiber dimensions after the treatment in environmental chamber. Current dimensional measurement is carried out in Acoustic AC (Tapping) mode with a Tap190DLC (BudgetSensors, Innovative Solutions Bulgaria Ltd.) probe [22] which has a resonant frequency of 190 kHz and force constant of 48 N/m. In AFM, a large area of 5 μm $\times$ 5 μm is scanned initially in order to locate the nanofibers. As mentioned in the fabrication methodology, the nanofibers are grown on a patterned Ni dots with a spacing of 1 μm. Scan images generated from AFM and SEM are shown in Fig. 2. Standing carbon nanofibers at spacing of 1 μm are clearly seen in the figure. Once the nanofibers are identified, substrate is rescanned to shrink the area to 2 μm $\times$ 2 μm in order to accurately measure the nanofiber dimensions. At this point, an arbitrary cross-section line is drawn over one nanofiber in the scanned image. This generates a 2-D graph as shown in Fig. 2(b) of the nanofiber, from which the fiber dimensions are obtained. As shown in the Fig. 2(b), the distance between the bases of the curve is the diameter of the nanofiber while the distance between the base and apex is the height of the nanofiber. In order to understand further, the 2-D image is converted to 3-D image using the AFM tool PicoImage. Fig. 2(c) shows a 3-D image obtained from the 2-D scan image of Fig. 2(a). From the 3-D image, evenly spaced vertically aligned and standing carbon nanofibers are clearly seen. From the 3-D image, the shape of the nanofibers can be clearly seen from all directions, and thus, temperature effect on the shape of the nanofiber can be realized. Fig. 2(d) shows the SEM image of the nanofibers scanned using a Philips SEM at 30 keV. Nanofibers are clearly seen as the white dots in the black background. Twenty measurements are taken after each exposure to environmental chamber.

2) AFM-Based Nanoindentation: In order to estimate Young's modulus, an important mechanical property of carbon nanofibers (CNFs), the atomic force microscope is used to scan

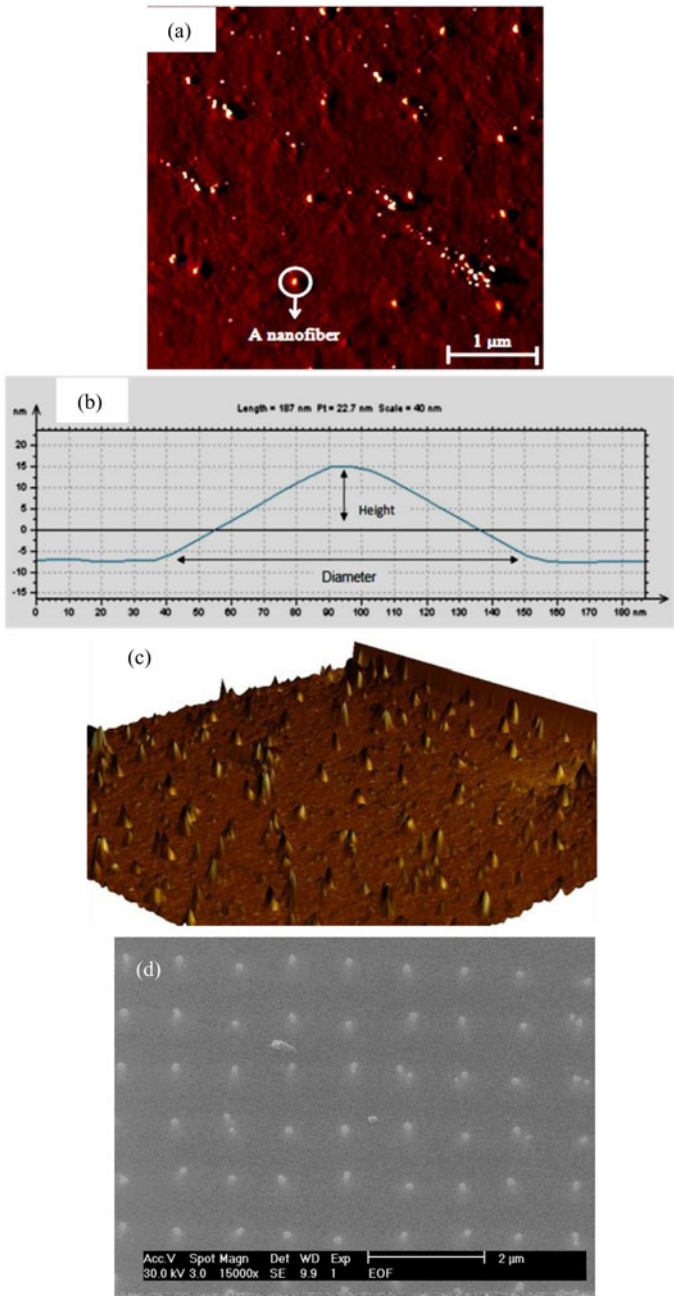

Fig. 2. AFM and SEM scan images of nanofibers. (a) 2-D scan image of the nanofibers generated by AFM. (b) Graph obtained by drawing a traversal across the nanofiber. (c) 3-D scan image of the nanofibers generated by the AFM. (d) SEM scan image of the nanofibers showing the evenly spaced CNFs.

the vertically aligned carbon nanofibers (VACNFs). After locating VACNFs by scanning a 5 μm $\times$ 5 μm square on the nanoelectrode arrays under Acoustic AC Mode, the AFM is utilized to perform nanoindentation on the located VACNFs. The AFM probe [22] is made of silicon with 15-nm-thick diamond-like-carbon coating and has an approximate conical shape, which has a half cone angle α of about 25° depicted in Fig. 3. Its force constant and resonant frequency is 48 N/m and 190 kHz, respectively. The tip diameter is less than 30 nm while the diameter of the fibers ranges from 110 nm to 250 nm. Thus, the Sneddon model [23] (cone-on-flat) as shown in Fig. 3(b) is employed

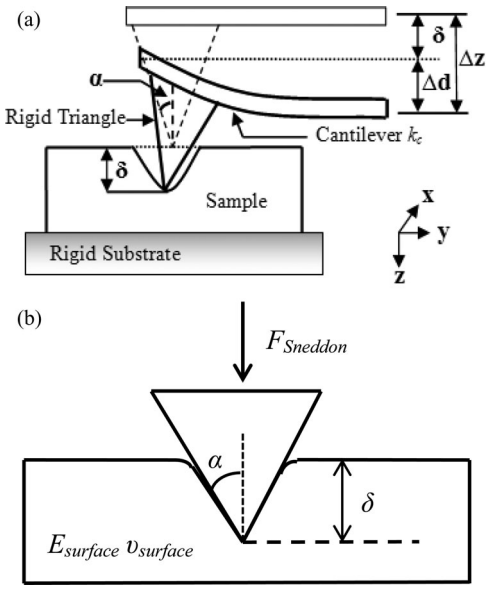

Fig. 3. Schematic for AFM-based nanoindentation: (a) illustration of z-axis movement, cantilever deflection, and indentation distance; and (b) Sneddon model.

to approximate this indentation process assuming the diamond-like-carbon coated probe is a rigid indenter. The relationship between the indentation force F_{Sneddon}, indentation distance δ, Poisson's ratio υ, and Young's modulus E_{sample} of the fibers (sample) is described as in the following equation:

$$F_{\mathrm{Sneddon}} = \frac{2}{\pi} \frac{E_{\mathrm{sample}}}{\left(1 - \nu_{\mathrm{sample}}^2\right)} \cot(\alpha)\, \delta^2. \tag{1}$$

The force curve of the indentation force F_{Sneddon} versus the indentation distance δ can be obtained from AFM-based nanoindentation. Then, the relation of F_{Sneddon} to δ^2 can be further derived and plotted. The slope $F_{\mathrm{Sneddon}}/\delta^2$ will be approximated using linear curve fit. Poisson's ratio, υ of the carbon nanofibers is assumed to be 0.06, which is Poisson's ratio of Carbon Nanotubes. Therefore, the only unknown variable left in (1) is E_{sample}, and can be computed easily by algebraic manipulation. (2) describes the relationship between the piezo scanner movement in z-axis Δz, the cantilever deflection Δd and δ, and (3) shows how to determine the indentation force, where k_c is the force constant of the cantilever

$$\Delta z = \Delta d + \delta \tag{2}$$

$$F = k_c \times \Delta d \tag{3}$$

III. Results and Discussion

A. Dimensional Measurement and Data Analysis

Fig. 4 shows the 3-D images of VACNFs generated from PicoImage after exposed to different subzero temperatures. As seen from the 3-D images, there is no change to the shape of the nanofibers before and after treatment. For reliability, 20 measurements are recorded and averaged. Table I shows the average and standard deviation of nanofibers after exposure to

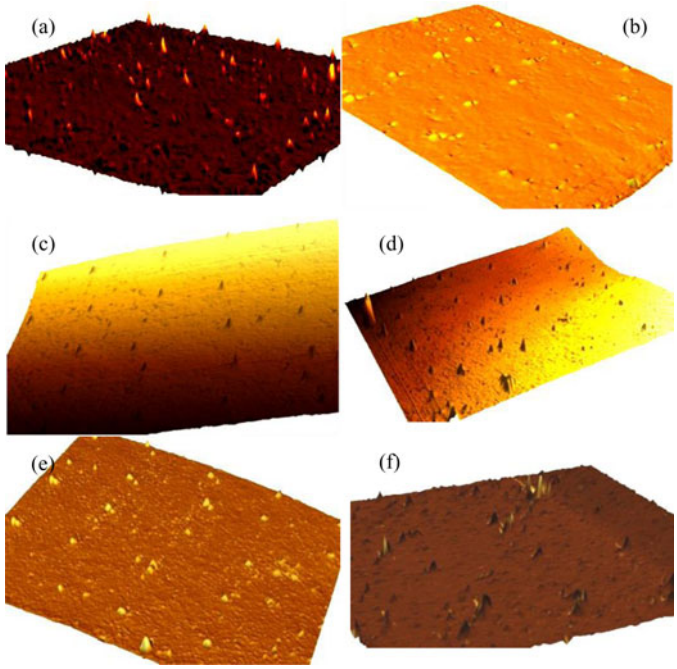

Fig. 4. Through F: 3-D scan images generated from the AFM-based PicoImage software after exposure to different temperatures. (a) −20 °C, (b) −30 °C, (c) −40 °C, (d) −50 °C, (e) −60 °C, and (f) −70 °C.

TABLE I
Average Diameter and Height of Nanofibers After Exposure to Extreme Temperatures

Temp (°C)	Average Height (nm)	Average Diameter (nm)	Standard Deviation of Height (nm)	Standard Deviation of Diameter (nm)
25	8.86	254	1.321	36.4
-20	5.25	189.5	0.939	27.5
-30	6.71	136.75	2.35	21.83
-40	5.44	112.77	1.28	15.36
-50	6.53	118.58	2.27	22.29
-60	5.99	173.2	1.172	17.03
-70	6.63	120.50	1.58	19.95

the extreme environments. From the Table I, it is clear that most of the nanofibers respond to the temperature changes. In most cases, the nanofiber dimensions decreased compared to that of room temperature.

B. Nanoindentation Analysis

The nanoelectrode arrays are scanned to locate VACNFs, and Fig. 2(a) shows the VACNFs that are treated in the environmental chamber at −70 °C for 30 min. The tip is then positioned on the top of one of the located fibers followed by a sweep of amplitude versus distance in vertical direction. Thus, the raw data of indenting a nanofiber are obtained as shown in Fig. 5(a), where "amplitude" describes Δd and "Z" presents Δz. In order to convert the amplitude in V into the cantilever deflection in nanometer (nm), calibration of sensitivity is necessary. Before scanning the nanoelectrode arrays, the same tip is used

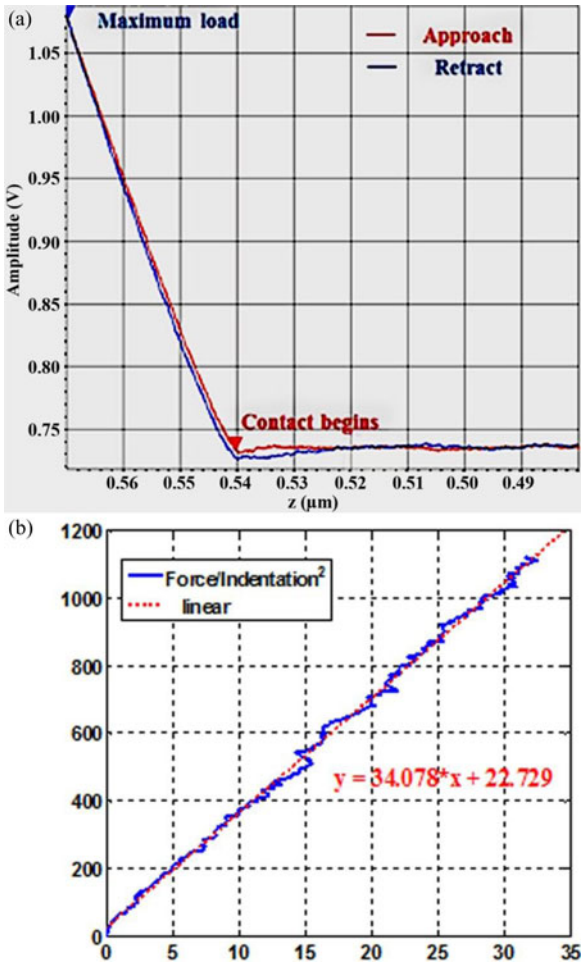

Fig. 5. (a) Amplitude Displacement curve obtained by nanoindentation. (b) Force F versus Indentation δ^2 generated from the raw data of nanoindentation.

to indent a mica disc surface 5 times. During this indentation period, the mica surface is assumed to be rigid, which indicates $\delta = 0$. Hence, the deflection of the cantilever Δd equals to the vertical displacement Δz, which is controlled by user when an indentation sweep is engaged.

Therefore, the sensitivity is obtained, and its mean value is calculated to be 68.5 nm/V with a standard deviation of 0.55 nm/V. With this sensitivity, the relation between the force and the indentation distance is obtained. Furthermore, the slope of force versus δ^2 is approximated by a linear fit as shown in Fig. 5(b). The linear fit provides the slope approximation, which is 34.078 nN/nm^2. Finally, this slope is substituted in (1) to compute value of the Young's modulus, $E_{\mathrm{VACNF}} = 23.9628$ GPa. Table II shows the results of E_{VACNFs} at different temperature treatments.

C. Discussion

1) Dimensional Measurement: From the current dimensional results, it is imperative that the dimensions of the CNFs are widely affected by the changes in temperatures. This is critically important because of the fact that most materials properties at nanoscale depend on the dimensions as well. Our particular interest lies in changes to the height of the nanofibers compared to the diameter as the side walls of the nanofibers are passivated by the silicon dioxide (SiO_2), and it leads to much more complex material behavior. Furthermore, it has been reported that the main problem with VACNF based sensor is that large variations in fiber height and overall fiber density will fluctuate the sensitivity of the sensor, which is the key to the reproducibility of sensor [21]. From the current dimensional results, it is observed that the nanofiber height decreases with the temperature when compared with the original room temperature. But in the subzero range, the height almost remained constant near to 6 nm.

TABLE II
YOUNG'S MODULUS CALCULATED FROM THE NANOINDENTATION DATA FOR THREE DIFFERENT FIBERS AFTER THE EXPOSURE TO EXTREME TEMPERATURE ENVIRONMENTS

Temp (°C)	Sample 1	Sample 2	Sample 3	Mean	Std dev
Room	511.82	1240.43	1010.68	920.98	372.50
-20	44.03	124.80	50.76	73.19	44.82
-30	70.36	64.41	80.86	71.88	8.33
-40	59.18	50.89	40.53	50.20	9.35
-50	37.66	34.22	55.07	42.32	11.17
-60	41.01	40.67	30.22	37.30	6.13
-70	23.54	20.84	26.86	25.09	1.67

All dimensions are in GPa.

2) Mechanical Properties Measurement: Besides the height of VACNFs, the other critical factor regarding the sensing ability is the density of fibers. Materials usually become more vulnerable at low temperatures. To investigate the mechanical properties of VACNFs at extreme temperatures become necessary as fibers are promising to work in space. Fibers, that lose their stiffness significantly, may no longer function as sensing elements. Mechanical properties of the nanofibers exposed to extreme environments are studied in detail. Young's moduli of the nanofibers are calculated at different temperatures. We obtained Young's modulus of 920 $\pm$ 372.5 GPa for nanofibers at room temperature. These values are in accordance with Young's modulus of multiwalled carbon nanotubes (MWCNTs) calculated from the prior experimental works [24], [25]. However, Young's modulus of the VACNFs fall drastically as the substrate is exposed to subzero temperatures. It is also imperative from the Table II that Young's modulus of the fiber almost reduced by 20 fold at subzero temperature range. Moreover, Young's modulus of the nanofibers decreases linearly as temperature changes in the subzero range. Fig. 6 shows Young's modulus plotted against temperature. With a 95% linear curve fit, regression line equation is calculated and it is given in equation (4) as follows. In statistics, coefficient of determination, R^2, or coefficient of correlation R are measures of linear fit. R^2 varies between 0 and 1 with 1 being the best fit and 0 being the worst fit. As depicted in Fig. 6, Young's versus temperature fit (red dashed line) has R^2 of 0.935 proving that the linear fit is the best fit for the obtained data for $-70\ ^{\circ}\mathrm{C} \leq \mathrm{T} \leq -20\ ^{\circ}\mathrm{C}$. Thus, from the equation, VACNFs will lose their complete stiffness at a temperature lower

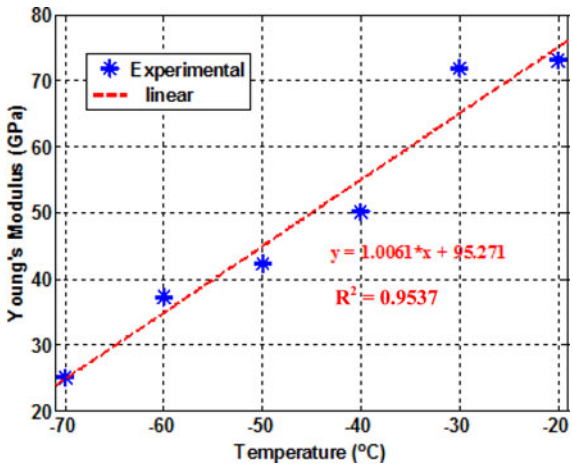

Fig. 6. Young's moduli versus temperatures.

than $-93.68\ ^{\circ}\mathrm{C}$

$$E_{\mathrm{VACNF}} = 1.0061 \times T + 95.271. \tag{4}$$

IV. Conclusion

From the current experimental results it can be inferred that the VACNFs lose their stiffness at temperatures lower than $-93.68\ ^{\circ}\mathrm{C}$. It is also observed that there is a decrease in diameter of the nanofibers compared to the room temperature while the height of the nanofiber remained constant in the subzero range. For the first time, AFM-based nanoindentation is used for the calculation of the mechanical properties of the nanofibers and Sneddon model is effectively used for obtaining Young's modulus of the nanofibers.

Acknowledgment

The authors would like to express their sincere gratitude to Dr. J. Koehne of NASA Ames research center for supplying the chips and for her timely guidance.

References

[1] J. W. G. Wildoer, L. C. Venema, A. G. Rinzler, R. E. Smalley, and C. Dekker, "Electronic structure of atomically resolved carbon nanotubes," *Nature*, vol. 391, pp. 59–62, 1998.

[2] T. W. Odom, J. L. Huang, P. Kim, and C. M. Lieber, "Atomic structure and electronic properties of single-walled carbon nanotubes," *Nature*, vol. 391, pp. 62–64, 1998.

[3] M. Burghard, "Electronic and vibrational properties of chemically modified single-wall carbon nanotubes," *Surf. Sci. Rep.*, vol. 58, pp. 1–109, 2005.

[4] S. Iijima, "Helical microtubules of graphitic carbon," *Nature (London)*, vol. 354, pp. 56–58, 1991.

[5] K. Balasubramanian and M. Burhard, "Biosensors based on carbon nanotubes," *Anal. Bioanal. Chem.*, vol. 385, pp. 452–468, 2006.

[6] J. Wang, M. Li, Z. Shi, N. Li, and Z. Gu, "Electrocatalytic oxidation of norepinephrine at a glassy carbon electrode modified with single wall carbon nanotubes," *Electroanal*, vol. 14, pp. 225–230, 2002.

[7] Z. Wang, J. Liu, Q. Liang, Y. Wang, and G. Luo, "Carbon nanotube-modified electrodes for the simultaneous determination of dopamine and ascorbic acid," *Analyst*, vol. 127, pp. 653–658, 2002.

[8] Y. Tu, Y. Lin, and Z. F. Ren, "Nanoelectrode arrays based on low site density aligned carbon nanotubes," *Nano Lett.*, vol. 3, pp. 107–109, 2003.

[9] Y. Lin, F. Lu, and J. Wang, "Disposable carbon nanotube modified screen-printed biosensor for amperometric detection of organophosphorus pesticides and nerve agents," *Electroanal (Invited, Spec. Issue: Nanotechnol.)*, vol. 16, pp. 145–149, 2004.

[10] Y. Lin, F. Lu, Y. Tu, and Z. F. Ren, "Glucose biosensor based on carbon nanotube nanoelectrode ensembles," *Nano Lett*, vol. 4, no. 2, pp. 191–195, 2004.

[11] J. K. Campbell, L. Sun, and R. M. Crooks, "Electrochemistry using single carbon nanotubes," *J. Amer. Chem. Soc.*, vol. 121, pp. 3779–3780, 1999.

[12] B. R. Azamian, J. J. Davis, K. S. Coleman, C. B. Bagshaw, and M. L. H. Green, "Bioelectrochemical single-walled carbon nanotubes," *J. Amer. Chem. Soc.*, vol. 124, pp. 12664–12665, 2002.

[13] C. V. Nguyen, L. Delzeit, A. M. Cassell, J. Li, J. Han, and M. Meyyappan, "Preparation of nucleic acid functionalized carbon nanotube Arrays," *Nano Lett.*, vol. 2, pp. 1079–1081, 2002.

[14] J. Li, H. T. Ng, A. Cassell, W. Fan, H. Chen, Q. Ye, J. Koehne, J. Han, and M Meyyappan, "Carbon nanotube nanoelectrode array for ultrasensitive DNA detection," *Nano Lett.*, vol. 3, pp. 597–602, 2003.

[15] J. Z Xu, J. J. Zhu, Q. Wu, Z. Hu, and H. Y. Chen, "An amperometric biosensor based on the coimmobilization of horseradish peroxidase and methylene blue on a carbon nanotubes modified electrode," *Electroanal*, vol. 15, pp. 219–224, 2003.

[16] S. B. Sinnott and R. Andrews, "Carbon nanotubes: synthesis, properties and applications," *Crit. Rev. Solid State Mater. Sci.*, vol. 26, pp. 145–249, 2001.

[17] F. Schedin, A. K. Geim, S. V. Morozov, E. W. Hill, P. Blake, M. I. Katsnelson, and K. S. Novoselov, "Detection of individual gas molecules adsorbed on graphene," *Nature Mater.*, vol. 6, pp. 652–655, 2007.

[18] U. Tisch and H. Haick, "Nanomaterials for cross-reactive sensor arrays," *MRS BULLETIN*, vol. 35, pp. 797–803, 2010.

[19] (07/06/2011). [Online]. Available: "http://www.nasa.gov/centers/ames/research/technology-onepagers/gas_detection.html"

[20] E. Kolawa, "Extreme Environment technologies for future space science missions," NASAReport, Sep. 19, 2007.

[21] P. U. Arumugam, H. Chen, S. Siddiqui, J. A. P. Weinrich, A. Jejelowo, J. Li, and M. Meyyappan, "Wafer-Scale fabrication of patterned carbon nanofiber nanoelectrode arrays: A route for development of multiplexed, ultrasensitive disposable biosensors," *Biosensors Bioelectronics*, vol. 24, pp. 2818–2824, 2009.

[22] AFM probe model: Tap190DLC, BudgetSensors, Innovative Solutions Bulgaria Ltd., Sofia, Bulgaria. (2013). [Online]. Available: http://www.budgetsensors.com/tapping_mode_afm_probes_long_cantilever_dlc.html.

[23] I. N. Sneddon, "The relation between load and penetration is the axisymmetric boussinesq problem for a punch of arbitrary profile," *Int. J. Eng. Sci.*, vol. 3, no. 1, pp. 47–57, 1965.

[24] M.-F. Yu, O. Lourie, M. J. Dyer, K. Moloni, T. F. Kelly, and R. S. Ruoff, "Strength and breaking mechanism of multiwalled carbon nanotubes under tensile load," *Science*, vol. 287, no. 5453, pp. 637–640, 28 Jan. 2000, Bibcode 2000Sci. . .287..637Y.

[25] B. Peng, M. Locascio, P. Zapol, S. Li, S. L. Mielke, G. C. Schatz, and H. D. Espinosa, "Measurements of near-ultimate strength for multiwalled carbon nanotubes and irradiation-induced crosslinking improvements," *Nature Nanotechnol.*, vol. 3, pp. 626–631, 2008.

Zhuxin Dong (S'07–M'13) received the B.E. degree in biomedical engineering from the Shenyang University of Technology, Liaoning, China, in 2005, and M.Phil. degree in mechanical and automation engineering from the Centre for Micro and Nano Systems (CMNS), The Chinese University of Hong Kong (CUHK), in 2007, where he was member of 3-D Digital Pen Team, and the Ph.D. degree in mechanical engineering from the University of Arkansas, Fayettevill, AR, USA, in 2012.

He is currently a Postdoctoral Research Associate in Na Lab, Department of Civil and Environmental Engineering and Earth Sciences, University of Notre Dame, Notre Dame, IN, USA. His research interest includes calibration and application of MEMS-based μIMU for human motion sensing and recognition, application of nanomaterials-based electrical devices, AFM-related measurement and manipulation, and micro fabrication.

Uchechukwu C. Wejinya (S'99–M'07) received the B.S. and M.S. degrees in electrical and computer engineering and the Ph.D. degree in electrical engineering all from Michigan State University, East Lansing, MI, USA, in 2000, 2002, and August 2007, respectively.

After completing the M.S. degree, he was with General Motors research and development center where he conducted research on Magneto-Rheological Fluid (MRF) clutch system before returning to graduate school. After completing the Ph.D. degree, he held a Postdoctoral Research Position in the Department of Electrical and Computer Engineering at Michigan State University. In February 2008, he joined the Department of Mechanical Engineering, University of Arkansas, where he is currently an Assistant Professor. His research interests include mechatronics with emphasis on nanotechnology–nanomaterials for nanosensors including biosensors, chemical; nanoelectronics; control systems design and application, robotics, electronics, microtools for handling and manufacturing of micro- and nanodevices, and modeling and simulation of micro- and nanostructures. He is the author and co-author of more than 70 conference and journal articles, and has presented at several national and international conferences. He also holds 2 U.S. patents.

Dr. Wejinya served on the administrative committee of IEEE Nanotechnology Council (NTC) from 2010 to 2012. He has given more than 15 invited talks nationally and internationally in his young career. He was among the first group of USA graduate students to participate in the National Science Foundation, East Asia Pacific Summer Institute in Beijing, China, in 2004 where he conducted research at the Chinese Academy of Sciences, Institute of Automation. In 2010, he received the prestigious Chinese Academy of Sciences Fellowship for Young International Scientist Award.He is a member of ASME and NSBE.

Siva Naga Sandeep Chalamalasetty (S'10–M'12) received the B.Tech. degree in biotechnology from Andhra University, Andhra Pradesh, India, in 2008, and the Master's degree in microelectronics and photonics from the University of Arkansas, Fayetteville, USA, in 2011.

He is currently with Micron Technology Inc., Manassas, VA, USA. Upon completion of his Bachelors, he was a Mathematics Instructor for eight months before returning back to School to complete his MS/PhD. His research interests include microfluidics for drug discovery and drug delivery, Bio-MEMS, micro/nano systems for ultrafast sensing using CNT/Graphene layers and material characterization.

M. Meyyappan (M'89–SM'96–F'04) received the Ph.D. degree in chemical engineering from Clarkson University, Potsdam, New York, USA, in 1984.

He is currently the Chief Scientist for Exploration Technology at the Center for Nanotechnology, NASA Ames Research Center, Moffett Field, CA, USA. Until June 2006, he was the Director of the Center for Nanotechnology as well as Senior Scientist. He is a founding member of the Interagency Working Group on Nanotechnology (IWGN) established by the Office of Science and Technology Policy. The IWGN is responsible for putting together the National Nanotechnology Initiative. He has authored or co-authored more than 190 articles in peer-reviewed journals and made more than 200 Invited/Keynote/Plenary Talks in nanotechnology subjects across the world. His research interests include carbon nanotubes and various inorganic nanowires, their growth and characterization, and application development in chemical and biosensors, instrumentation, electronics and optoelectronics.

Dr. Meyyappan is a Fellow of the Electrochemical Society, AVS, the Materials Research Society (MRS), and the California Council of Science and Technology. In addition, he is a member of the American Society of Mechanical Engineers (ASME) and the American Institute of Chemical Engineers (AIChE). He is currently the IEEE Nanotechnology Council Distinguished Lecturer on Nanotechnology, IEEE Electron Devices Society (EDS) Distinguished Lecturer, and was ASME's Distinguished Lecturer on Nanotechnology (2004–2006). He served as the President of the IEEE's Nanotechnology Council during 2006–2007. For his contributions and leadership in nanotechnology, he has received numerous awards including: a Presidential Meritorious Award; NASA's Outstanding Leadership Medal; Arthur Flemming Award given by the Arthur Flemming Foundation and the George Washington University; IEEE Judith Resnick Award; IEEE-USA Harry Diamond Award; AIChE Nanoscale Science and Engineering Forum Award. For his sustained contributions to nanotechnology, he was inducted into the Silicon Valley Engineering Council Hall of Fame in February 2009. For his educational contributions, he has received: Outstanding Recognition Award from the NASA Office of Education; the Engineer of the Year Award (2004) by the San Francisco Section of the American Institute of Aeronautics and Astronautics; IEEE-EDS Education Award; IEEE- Educational Activities Board Meritorious Achievement Award in Continuing Education.